ELSEVIER

Approximate analytical model for two-phase solidification problem in a finned phase-change material storage

Piia Lamberg*

Olof Granlund Oy, Malminkaari 21, PO Box 407, 00103 Helsinki, Finland

Abstract

During the phase change in a phase-change material (PCM) storage system, the solid–liquid interface moves away from the heat transfer surface and the surface heat flux decreases due to the increasing thermal resistance of the molten or solidified medium. Heat-transfer enhancement techniques such as fins and honeycombs have to be used to increase the heat-transfer fraction in the store. The purpose of this paper is to develop a simplified analytical model which predicts the solid–liquid interface location and temperature distribution of the fin in the solidification process with a constant end-wall temperature in the finned two-dimensional PCM store. The storage is initially in a liquid state and its temperature is greater than the solidification temperature of the PCM. The analytical results are compared to the numerical results calculated using the heat-capacity method. The results show that the analytical model gives a satisfactory estimation for the fin temperature and the solid–liquid interface when the length-to-height ratio (λ) of the storage cell is smaller than 6.0 and the fin length is smaller than 0.06 m. The error made in the fraction of solidified PCM is $\pm 10\%$ when the analytical model is used rather than the two-dimensional numerical model.
$\copyright$ 2003 Elsevier Ltd. All rights reserved.

Keywords: PCM; Analytical model; Solidification problem; Finned PCM storage

1. Introduction

In the late 19th century, J. Stefan formulated the solution for finding the temperature distribution and freezing-front history of a solidifying slab of water. Since

---

* Corresponding author. Tel.: +358-9-3510-3387; fax: +358-9-3510-3424.
 E-mail address: piia.lamberg@granlund.fi (P. Lamberg).

Nomenclature

c_p	heat capacity (J kg^{-1} K^{-1})
D	half thickness of the fin (m)
h	enthalpy (J)
k	heat conductivity (W m^{-1} K^{-1})
l	length (m)
L	latent heat of fusion (J kg^{-1})
S	location of the phase-change interface (m)
T	temperature (°C)
ΔT_m	solidification temperature-range (°C)
t	time (s)

Greek symbols

α	thermal diffusivity (m^2 s^{-1})
ρ	density (kg m^{-3})
ϵ	fraction of solidified PCM
λ	root of the transcendental equation
$\theta = T_f - T$	dimensionless temperature-distribution
ν	$\dfrac{k_s}{S_y (\rho c_p)_f D}$
κ	$\dfrac{k_s}{(\rho c_p)_f}$

Subscripts and superscripts

eff	effective
f	fin
i	initial
l	liquid
m	solidification
s	solid
w	wall
x	x-direction
y	y-direction

then, particularly in the last 30 years, the problem bearing his name has been extended to include such complex phenomena as the solidification of alloy systems and supercooling. Different materials and their material properties, especially the latent heat of fusion, have been studied intensively to find out which materials can be used for storing energy as latent heat rather than as sensible heat.

The most commonly used PCMs in storing energy are paraffins, salts and salt hydrates and fatty acids. The PCM stores and releases large amounts of heat when

changing its phase. The advantage of PCM storage compared to sensible heat-storage systems, such as water storage, is its potential to store large amounts of heat with only a small temperature swing. However, PCMs have some disadvantages, such as the low heat-conductivity of the material. The heat-conductivity of paraffins varies between 0.1 and 0.2 W m^{-1} K^{-1} and that of salt hydrates between 0.4 and 0.6 W m^{-1} K^{-1}, depending on the material [1].

During phase change in PCM storage systems, the solid-liquid interface moves away from the heat-transfer surface. During this process, the surface heat-flux decreases due to the increasing thermal resistance of the molten or solidified medium. The decreasing heat-transfer rate calls for the usage of heat-transfer enhancement techniques. Some applications require heat to be charged at a faster rate while others require heat to be discharged at a faster rate [2].

It is possible to enhance the internal heat-transfer of PCM storage with fins, metal honeycombs, metal matrices (wiremesh), lessing rings, high-conductivity particles or graphite [2,3]. Heat transfer during solidification in a store with internal fins has been studied numerically and experimentally by many authors.

Heat-transfer enhancement in the solidification process in a finned PCM store with a heat exchanger was studied numerically and experimentally by Stritih et al. [4]. The enthalpy method was used as a numerical method to calculate the temperature distribution of finned PCM storage. They concluded that the biggest influence on the heat transfer in the solidification process is the distance between the fins. The thickness of the fin is not as influential.

Humphries et al. [5] studied numerically a rectangular phase-change store containing fins used as a heat-transfer enhancement using the enthalpy method. The data were generated over a range of realistic sizes, material properties and different kinds of thermal boundary-conditions, resulting in a design handbook for phase-change energy storage.

Enhanced heat-conduction in phase-change thermal-energy storage devices was studied by Henze et al. [6]. They presented a simplified numerical model based on a quasi-linear, transient, thin-fin equation, which predicts the location of the solid–liquid interface as a function of time. In this work, the two-dimensional problem was simplified to a one-dimensional problem.

The exact analytical solution for the solid–liquid interface location in two-dimensional PCM store with internal fins is not found. However, Lamberg et al. simplified the two-dimensional heat-transfer problem to a one-dimensional one and derived an analytical solution for the melting process in a semi-infinite PCM store with internal fins [7]. The initial temperature of the store was assumed to be the melting temperature of the PCM. They found an exact solution for the temperature distribution of the fin and for the solid–liquid interface location with a constant end-wall temperature. The analytical results were compared to the numerical results and they showed good agreement.

Lamberg et al. continued to study the solidification process with constant end-wall temperature boundary-conditions in a finned PCM store [8]. Initially, the store was at the PCM's solidification temperature. The analytical results were compared to the numerical results and they showed that the analytical model gives a

good approximation for the temperature of the fin and the solid–liquid interface location.

This paper continues the one-dimensional analytical approach of the two-dimensional heat-transfer problem in finned PCM store in cases where the store is initially at a higher temperature than the PCM's solidification temperature. The analytical model predicts the solid–liquid interface location and the temperature distribution of the fins during the solidification process in a finned PCM store. In addition to the one-dimensional analytical approach, the problem is also solved numerically in two-dimensions using the effective heat capacity method. The calculation with the effective heat-capacity method is carried out using a program called FEMLAB, which is a simulation package that solves systems and coupled equations through the finite-element method in one-, two- and three-dimensions [9].

The main advantages of the analytical model are simplicity and short computation-times. These features can be valuable in certain situations, such as in the pre-design stage of the store. Absolute precision is not important in such a situation but the speed of the calculation is, so enabling comparison of several alternatives to the storage dimension within a reasonable time.

2. A finite PCM store with internal fins

In this work, the solidification process in a finite two-dimensional PCM store with internal fins is studied (Fig. 1). The PCM store consists of a metal housing with internal straight metal fins. The store is filled with a phase-change material. Initially the store is at a uniform temperature T_i. The PCM is in the liquid phase and its initial-temperature is higher than its solidification temperature ($T_i > T_m$). The
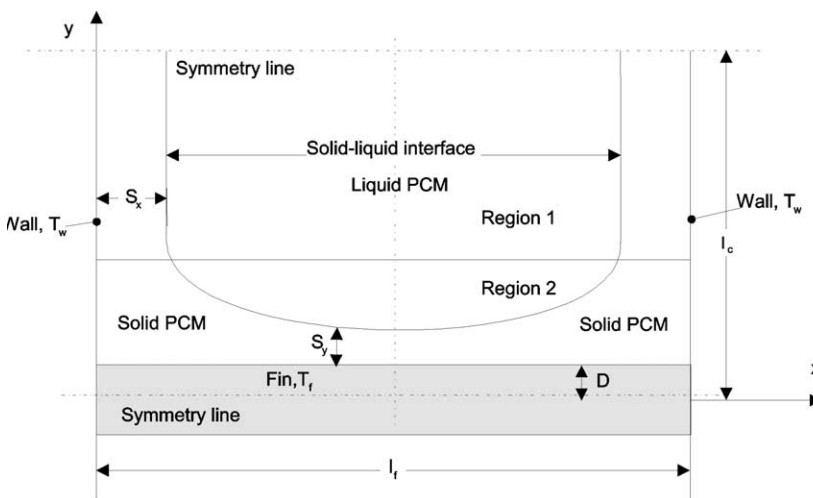
Fig. 1. The symmetry cell of PCM store with an internal fin.

temperature of the end-walls of the store are instantaneously lowered and kept at the temperature T_w ($T_w < T_m$).

The liquid PCM starts to cool down and releases heat; first as sensible heat in the iquid PCM, then as latent heat of fusion during the phase change and finally as sensible heat from the solid PCM until it reaches the temperature of the walls. The amount of latent heat is large compared to the sensible heat of the material when the temperature difference between the initial temperature and the end temperature of the store is small.

The main heat-transfer mode is conduction in the solidification process. Initially, natural convection exists in the liquid–solid interface due to the temperature difference in the liquid PCM. However, even very strong natural convection in the solid–liquid interface has a negligible effect on the solid–liquid interface position compared to the effect of heat conduction in the solid PCM [10]. Heat released during cooling and the phase-change process transfers by conduction along the fins and through the phase change material from the solid–liquid interface to the end-walls. The PCM store is symmetrical in structure (Fig. 1). The dimensions of the store have a significant effect on the speed of the cooling and the solidification of the material.

When the cells aspect ratio (the length of the fin divided by the height of the cell)

$$\lambda = \frac{l_f}{l_c} \tag{1}$$

is much smaller than unity ($\lambda << 1$), the heat transfer occurs mainly in the x-direction. When λ is equal to unity, the heat transfers at the same rate in the x-direction as in the y-direction and when $\lambda >> 1$, the heat transfer is dominant in the y-direction.

The heat equation for the PCM and the enclosure with boundary and initial conditions can be written as

$$\frac{\partial T}{\partial t} = \frac{k}{\rho c_p}\left(\frac{\partial^2 T}{\partial x^2} + \frac{\partial^2 T}{\partial y^2}\right) \qquad\qquad , t > 0 \tag{2}$$

$$T(x, y, 0) = T_i \tag{3}$$

$$T(0, y, t) = T(l_f, y, t) = T_w \tag{4}$$

and the energy balance for the solid–liquid interface with the initial conditions is [11]:

$$k\left[\left(\frac{\partial T}{\partial y}\right)_s + \left(\frac{\partial T}{\partial y}\right)_l\right]\left[1 + \left(\frac{\partial S}{\partial x}\right)^2\right] = \rho L \frac{\partial S}{\partial t}\bigg|_{y=S} \qquad , t > 0 \tag{5}$$

$$S(x, 0) = 0 \tag{6}$$

where T is the temperature of the PCM or enclosure, t is time, c_p heat capacity, ρ density, k heat conductivity of the PCM or enclosure, L the latent heat of fusion, S the location of the solid-liquid interface, T_i the initial temperature and T_m the solidification temperature of the PCM. The subscript s denotes the solid PCM, l the liquid PCM and f the fin.

The problem is a classical Stefan-type problem, whose basic feature is that the regions in which the partial-differential equations apply are unknown and must be found as part of the solution of the problem. This amounts to a non-linearity of geometric nature even when the rest of the equations appear to be linear. Non-linearity is the source of difficulties and it destroys the validity of generally-used solving methods such as the superposition method and the separation of variables method [12]. Therefore, the analytical solution for this kind of two-dimensional heat-transfer problem with a phase change has not yet been found. However, it is possible to solve the problem quite easily with numerical methods such as the enthalpy method or the effective heat-capacity method.

3. One-dimensional analytical approach

The PCM store is symmetrical in structure (Fig. 1). The symmetry cell is divided into two regions. In region 1, the only heat sink is the constant temperature end-wall. Here the fin does not influence the solidification process. In region 2, both the wall and the fin transfer heat from the phase-change material to the environment.

Due to the non-linear, unsteady nature, several assumptions have been made to simplify the two-dimensional heat-transfer problem. The assumptions are the following:

- Initially the PCM is in a liquid state. Due the temperature difference and the buoyancy effect in the liquid PCM, natural convection exists in the liquid material. However, in a small PCM store, the effect of natural convection is assumed to be negligible. The sole heat transfer mode is assumed to be conduction.
- The solidification temperature (T_m) is assumed to be constant. In reality a phase-change material has a wider solidification range (ΔT_m) in which solidification occurs.
- The temperature distribution of the fin is considered to be one-dimensional in the x-direction because the fin is thin and the conductivity of the fin material is high.
- In region 1, heat transfer is one-dimensional only in the x-direction. The fin does not have an effect on heat transfer in this region.
- In region 2, the solid–liquid interface moves only one-dimensionally in the y-direction because the heat is mainly transferred through the fin to the environment.
- When the thermal diffusivity α of the PCM approaches zero ($\alpha = \frac{k}{\rho c_p} \approx 0$), it can be assumed that $\frac{\partial T}{\partial t} = 0$ and $T(x,t) = T_i$ in the liquid PCM. The sensible heat

of the liquid PCM is taken account in the enhanced latent heat term—$[L + c_l(T_i - T_m)]$ which slows down the freezing front [12]. Thus, the initial temperature of the PCM is the solidification temperature T_m instead of the initial temperature T_i. The enhanced latent-heat term slows down the freezing front which starts to move directly when $t > 0$ s.

• The initial temperature of the fin is also assumed to be T_m instead of T_i. In this approximation model, the solidification process is assumed to start immediately when the walls are imposed at a lower temperature. Therefore, the derived analytical model is limited to use for short, well-conductive fins in which the temperature decreases quickly from the initial temperature to the solidification temperature.

In region 1 the solidification can be handled as a one-dimensional single-phase Stefan problem [12]. The cooling of the PCM before the solidification process is taken into account in the enhanced latent-heat term—$[L + c_l(T_i - T_m)]$. The heat equation for a solid phase change material and for a solid–liquid interface with initial and boundary conditions can be written as:

$$\frac{\partial T_s}{\partial t} = \left(\frac{k}{\rho c_p}\right)_s \frac{\partial^2 T_s}{\partial x^2}, \qquad\qquad , t > 0 \qquad\qquad (7)$$

$$-\rho_s[L + c_l(T_i - T_m)]\frac{\partial S_x}{\partial t} = -k_s \frac{\partial T_s(S_x, t)}{\partial x} \qquad\qquad , t > 0 \qquad\qquad (8)$$

$$S_x(0) = 0 \qquad\qquad (9)$$

$$T_s(S_x, t) = T_m \qquad\qquad (10)$$

$$T_s(0, t) = T_s(l_f, t) = T_w \qquad\qquad (11)$$

where S_x is the location of the solid–liquid interface in the x-direction from the end wall as a function of time.

In region 2, the movement of the solid–liquid interface is assumed to occur only in the y-direction. The energy balance for the fin can be rewritten with the initial and boundary conditions as:

$$(\rho c_p)_f D \frac{\partial T_f}{\partial t} = k_f D \frac{\partial^2 T_f}{\partial x^2} - \frac{k_s}{S_y}(T_f - T_m) \qquad\qquad , t > 0 \qquad\qquad (12)$$

$$T_f(x, 0) = T_m \qquad\qquad (13)$$

$$T_f(0, t) = T_w \qquad\qquad (14)$$

$$T_f(l_f, t) = T_w \tag{15}$$

where S_y is the location of the solid–liquid interface in the y-direction from the fin. The heat equation for the phase-change material and for a solid–liquid interface with initial and boundary conditions can be written as:

$$\frac{\partial T_s}{\partial t} = \left(\frac{k}{\rho c_p}\right)_s \frac{\partial^2 T_s}{\partial y^2}, \qquad\qquad , t > 0 \tag{16}$$

$$-\rho_s[L + c_l(T_i - T_m)]\frac{\partial S_y}{\partial t} = -k_s \frac{\partial T_s(S_y, t)}{\partial x} \qquad\qquad , t > 0 \tag{17}$$

$$S_y(0) = 0 \tag{18}$$

$$T_s(S_y, t) = T_m \tag{19}$$

$$T_s(D, t) = T_f \tag{20}$$

To enable the solution of equations Eqs. (12)–(15) to be obtained, the following dimensionless variables are introduced:

$$\theta = T_f - T_m, \quad \nu = \frac{k_s}{S_y(\rho c_p)_f D} \quad \text{and} \quad \kappa = \frac{k_s}{(\rho c_p)_f}.$$

Eqs. (12)–(15) are rewritten by using the dimensionless variables.

$$\frac{\partial \theta}{\partial t} = \kappa \frac{\partial^2 \theta}{\partial x^2} - \nu\theta \qquad\qquad , t > 0 \tag{21}$$

$$\theta(\eta, 0) = 0 \tag{22}$$

$$\theta(0, \tau) = 1 \tag{23}$$

$$\theta(1, \tau) = 1 \tag{24}$$

In region 1, Eqs. (7)–(11) are solved with the quasistationary approximation method, which overestimates the location of the solidification front. However, the overestimation will compensate for the fact that the problem is handled one-dimensionally instead of two-dimensionally. The heat transfers much more slowly from

the storage to the environment in a one-dimensional case than in a two-dimensional case. The method consists of replacing the heat conduction equation with a steady-state equation $\frac{\partial^2 T}{\partial x^2} = 0$. The distance of the solid–liquid interface from the end wall is [12]

$$S_x = \sqrt{\frac{2k_s(T_w - T_m)t}{-\rho(L + c_l(T_i - T_m))}}. \tag{25}$$

In region 2, the solution for the dimensionless temperature of the fin is [7,13]

$$\theta = \frac{\cosh(x)\sqrt{v/\kappa}}{\cosh\left(l_f/2\sqrt{v/\kappa}\right)}$$
$$- \frac{4}{\pi e^{vt}} \sum_{n=0}^{\infty} \frac{(-1)^n e^{-\kappa(2n+1)^2\pi^2 t/(2l_f))}}{(2n+1)\left[1 + \left\{vl_f^2/((2n+1)^2\pi^2\kappa)\right\}\right]} \cos((2n+1)\pi x/l_f) \tag{26}$$

$$T_f = T_m + \theta(T_W - T_m). \tag{27}$$

Eqs. (16)–(20) are also solved with the quasistationary approximation method. The distance of the solid–liquid interface from the fin is [12]

$$S_y = \sqrt{\frac{2k_s(T_f - T_m)t}{-\rho(L + c_l(T_i - T_m))}}. \tag{28}$$

The temperature T_f of the fin and the distance S_y of the solid–liquid interface from the fin are solved from Eqs. (25)–(28).

4. Two-dimensional numerical approach

4.1. The accuracies of different numerical methods

In reality in phase-change situations, more than one phase-change interface may occur or the interfaces may disappear totally. Furthermore, the phase change usually happens in a non-isothermal temperature range. In such cases, tracking the solid-liquid interface may be difficult or even impossible. From the point of view of calculations, it is advantageous that the problem is reformulated in such a way that the Stefan condition is implicitly bound up in new forms of the equations and that equations [Eqs. (2)–(6)] are applied over the whole fixed domain.

The most commonly used numerical methods are the effective heat-capacity method and the enthalpy method. Lamberg et al. [14] have compared the numerical results calculated using the effective heat-capacity method and the enthalpy method

to experimental results achieved by using thermocouples mounted inside the PCM store. Two different stores were built and modelled, one with internal fins and one without fins. The PCM was initially in a solid state at a temperature of 10 °C in the store. The store was heated up from 10 to 40 °C and when the PCM reached the steady temperature, the store was cooled down back to 10 °C. The entire 10–40–10 °C cycle took about 2.5–3 h and it was repeated at least five times for each measurement. For each cycle, the temperature responses of either eight (storage with no fins) or 16 (finned storage) thermojunctions were recorded at one-minute intervals. The store without fins with the location of the measurement points are shown in Fig. 2.

The numerical calculations were performed using the effective heat-capacity method and with the enthalpy method using the FEMLAB program. In the effective heat-capacity method, two different solidification ranges $\Delta T_\mathrm{m} = 2$ °C and 7 °C were used.

In Fig. 3, the numerical and experimental results of the melting and solidification processes in the PCM store are presented. Eff2 and Eff7 denote the effective heat-capacity method with a solidification temperature range of between 2 °C and 7 °C, where Ent equals the enthalpy method and Exp the experiments at measurement point four (see Fig. 2) [14].

Firstly, the PCM starts to melt when the effective heat-capacity method with a wide temperature range is used. However, quite soon, the effect of natural convection makes uniform the temperature development of the PCM in all the numerical methods. All the numerical results follow quite well the experimental results for the temperature of the PCM.

During the solidification process, all the numerical methods give uniform results for the temperature of the PCM in the liquid state. When solidification begins, the effective heat-capacity method with a wide temperature-range gives nearly the same results as the enthalpy method, but differs from the results achieved with the effective heat-capacity method with a narrow phase-change range.

Lamberg et al. [14] concluded that the most precise numerical method is the effective heat-capacity method with a narrow solidification temperature-range $\Delta T_\mathrm{m} = 2$ °C (eff2). Thus, in this paper, the analytical results are compared to the numerical results calculated using the effective heat-capacity method with a narrow temperature range $\Delta T_\mathrm{m} = 2$ °C.

4.2. Effective heat-capacity method

The effective heat-capacity of the material (c_eff) is directly proportional to the stored and released energy during the phase change and also to the specific heat-capacity. However, it is inversely proportional to the width of the solidification temperature range, as can be seen in Eq. (29) [15]:

$$c_\mathrm{eff} = \frac{L}{(T_2 - T_1)} + c_\mathrm{p} \tag{29}$$

where T_1 is the temperature where the solidification begins and T_2 the temperature where the material is totally solidified.

Storage 1 Thermojunction	x mm	y mm
1	1.191	25.4
2	3.92	31.02
3	6.38	36.16
4	8.73	42.17
5	11.28	47.3
6	13.47	53.13
7	15.62	58.99
8	17.26	64.32
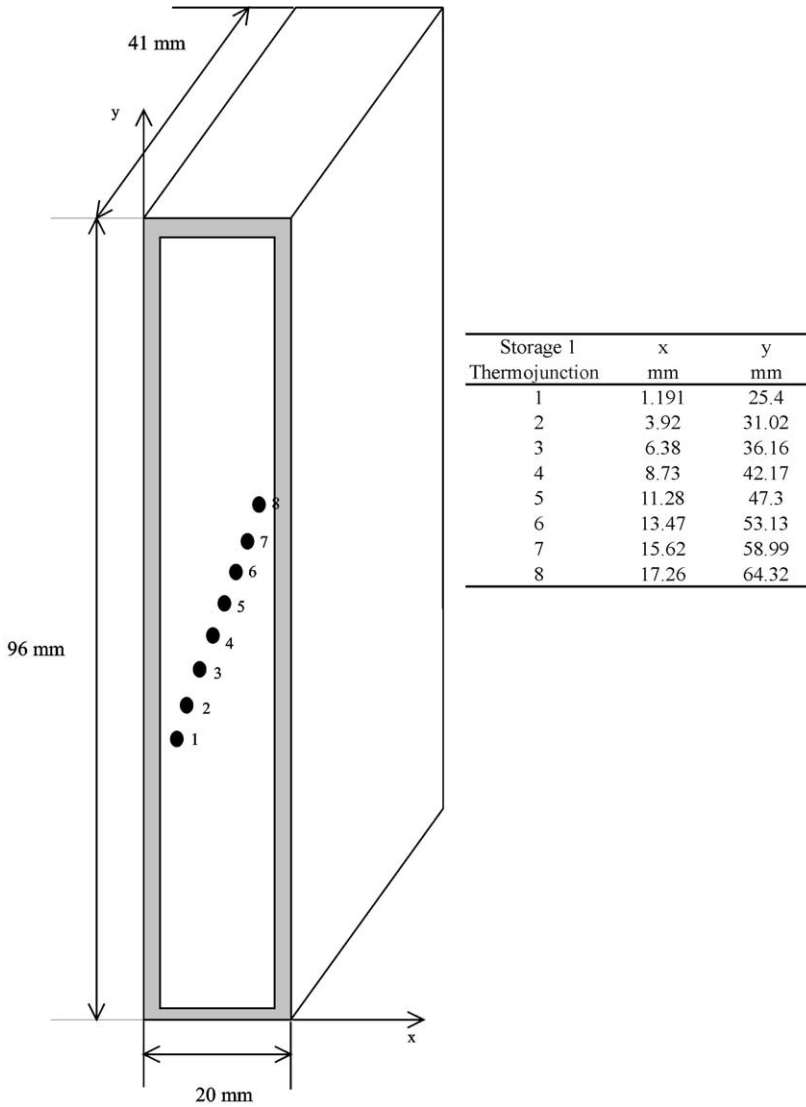
Fig. 2. PCM storage with placement of the thermojunctions.

The heat equation with initial and boundary conditions for the PCM and the fin is

$$\frac{\partial T}{\partial t} = \frac{k}{c_p \rho} \left(\frac{\partial^2 T}{\partial x^2} + \frac{\partial^2 T}{\partial y^2} \right) \qquad , t > 0 \qquad (30)$$

$$T(x, y, 0) = T_i \qquad (31)$$
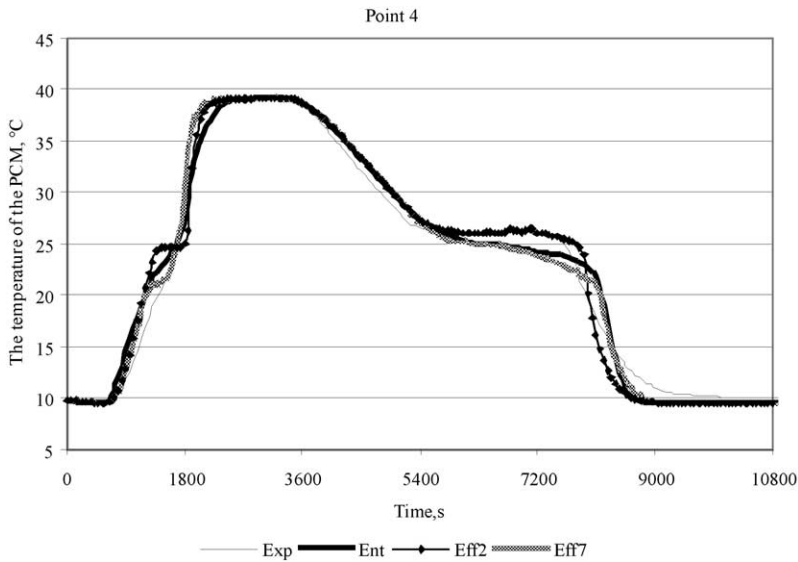
Fig. 3. The numerical and experimental results of melting and solidification processes in the PCM store.

$$T(0, y, t) = T(l_f, y, t) = T_w \tag{32}$$

where

$$c_p = \begin{cases} c_s, & T < T_1 \\ \dfrac{L}{(T_2 - T_1)} + c_p, & T_1 \leqslant T \leqslant T_2 \\ c_l, & T > T_2 \end{cases} \tag{33}$$

The effective heat-capacity method is valid for the phase-change material and for the fin except in Eq. (33). The latent heat term $\left(\frac{L}{(T_2-T_1)} + c_p \right)$ is ignored when the fin is taken into consideration. The numerical calculations are performed using the FEMLAB program [16].

5. Results

5.1. Test cases

The temperature distribution in the fin and the location of the solid–liquid interface is calculated using the derived one-dimensional analytical method and with the two-dimensional numerical effective heat capacity method. The results are compared with each other to find the accuracy and performance of the one-dimensional analytical approach and the solution.

Three test cases with different geometries are chosen. In the test cases the initial temperature of the store is 40 °C and the PCM is in the liquid state. The wall temperature is set at 10 °C. The phase-change material is paraffin and the fin material aluminium. The peak solidification temperature of the PCM is 25 °C. The physical properties of the phase change and the fin materials are shown in Table 1 [17]. The heat conductivity and the density of the paraffin are assumed to be constant.

The half thickness, D, of the fin has a constant value of 0.5 mm in all the test cases. Otherwise, the geometry of the store is varied in the different cases. The width-to-height ratio $\lambda = L_f/L_c$ is given the values 0.2, 3.0 and 5.0.

5.2. The temperature of the fin

The temperature of the fin is calculated using the derived analytical solution in Eqs. (25)–(28) and by using the effective heat-capacity method [Eqs. (30)–(33)]. In Fig. 4 the results in test case 1 are shown at time steps $t = 200$ s and 400 s.

When the fin is short, it achieves the end-wall temperatures quickly because of its better heat conductivity compared to the conductivity of the phase-change material. The temperature of the fin is a little higher in the analytical solution than in a numerical solution. However, the error made is small, approximately 0.05 °C at $t = 200$ s and 0.07 °C $t = 400$ s.

The temperature of the fin that was calculated using the analytical and numerical solution in case 2 is presented in Fig. 5.

At $t = 200$ s the temperature of the fin is higher in the numerical solution than in the analytical solution. In the derived analytical model, it has been assumed that the fin is initially at the same temperature as the PCM's solidification temperature. Therefore, at the beginning of the solidification process, it can be seen that the fin cools down too quickly in the analytical solution. The temperature difference between the analytical and the numerical solutions is 0.2 °C at $t = 200$ s. When $t = 400$ s, it can be noticed that the temperature difference between the analytical and the numerical solution diminishes and it is only 0.05 °C. Overall, the derived analytical model gives a quite good estimation for the temperature of the fin when compared to the numerical solution.

Table 1
Physical properties of the paraffin and the aluminium fin

Property	Paraffin	Aluminium fin
Density (ρ) (kg m^{-3})	770	2710
Heat conductivity (k) (Wm^{-1} K^{-1})	0.185	174
Heat capacity, liquid (c_p) (J kg^{-1} K^{-1})	2400	–
Heat capacity, solid (c_p) (J kg^{-1} K^{-1})	1800	935
Latent heat of fusion (L) (J kg^{-1})	124 098	–
Peak solidification temperature (T_m) (°C)	25	–
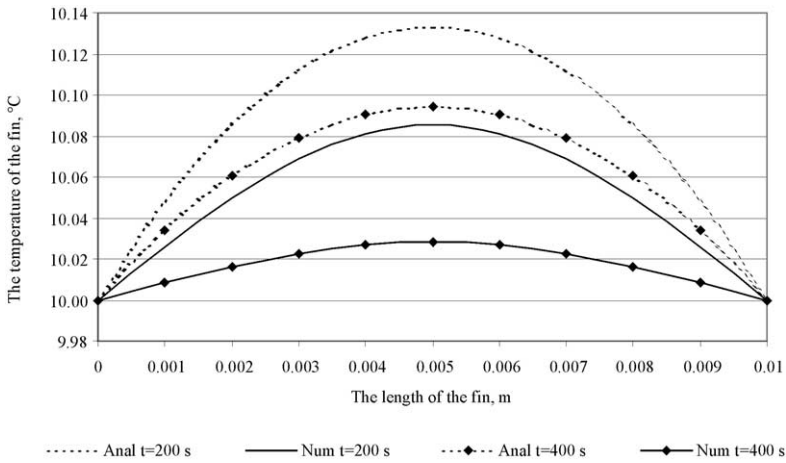
Fig. 4. The temperature of the fin in the PCM store in case 1 ($\lambda = 0.2$, $l_f = 0.01$ m, $l_c = 0.05$ m).
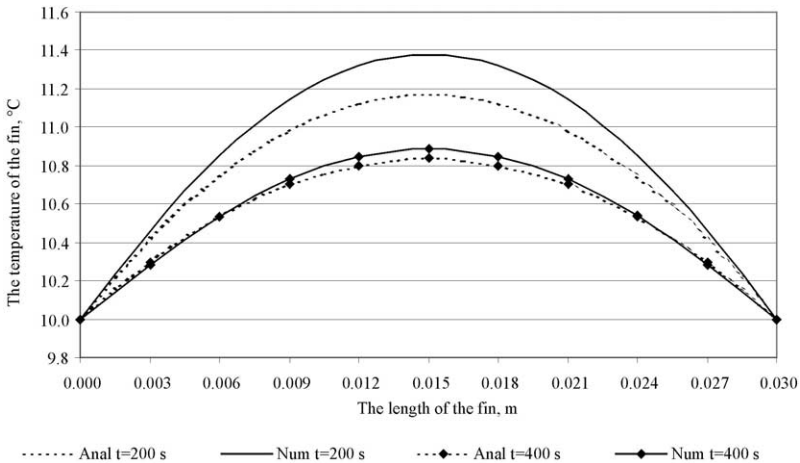
Fig. 5. The temperature of the fin in the PCM store in case 2 ($\lambda = 3$, $l_f = 0.03$ m, $l_c = 0.01$ m).

Fig. 6. presents the temperature of the fin in case 4 at $t = 300$ s and $t = 900$ s. The time steps are chosen to be higher in case 3 than in cases 1 and 2 because the solidification process takes more time when the fin is long.

The assumption that the fin is initially at the solidification temperature of the PCM was made in the analytical model. It is also possible to see the effect of this assumption in Fig. 6. The temperature of the fin is much smaller in the analytical solution than in the numerical solution. The temperature difference between the
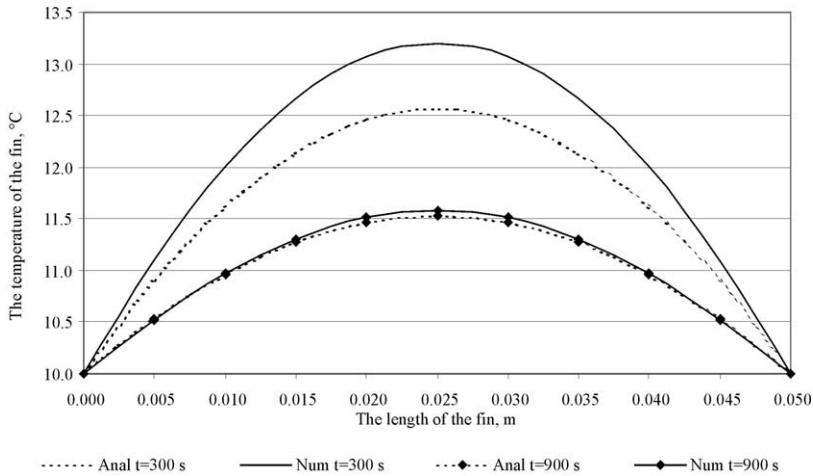
Fig. 6. The temperature of the fin in the PCM store in case 3 ($\lambda = 5$, $l_f = 0.05$ m, $l_c = 0.01$ m).

analytical and the numerical results is 1.5 °C at $t = 300$ s and 0.05 °C at $t = 900$ s. However, the temperature difference diminishes when the time increases.

5.3. The location of the solid–liquid interface

The solid–liquid interface in different cases is calculated using the derived analytical solution [Eqs. (25)–(28)] and also by using the effective heat-capacity method [Eqs. (30)–(33)]. In Fig. 7, the temperature distribution of the storage is shown and is calculated using the effective heat-capacity method with the FEMLAB program in cases 1, 2 and 3 at $t = 300$ s.

The location of the solid–liquid interface is defined from the temperature distribution of the store calculated using the effective heat capacity method by assuming that the interface is located for the temperature $T_m = 25$ °C.

In Fig. 8, the location of the solid–liquid interface in case 1 calculated using the analytical and numerical methods at $t = 200$ s and $t = 400$ s are presented.

The derived analytical model is one-dimensional in both the x- and the y-direction. In reality, the two-dimensional heat-transfer in the storage accelerates the solidification process. It is also possible to see this phenomenon in Fig. 8. The interface in the one-dimensional analytical approach moves more slowly than in the two-dimensional numerical approach. The quasistationary solution compensates to a degree for the lack of two-dimensional heat-transfer in the derived analytical method.

The difference in the solid–liquid interface calculated using the analytical and the numerical model is 0.09 mm in the x-direction and 2.08 mm in the y-direction at the time step $t = 200$ s and 0.5 mm in the x-direction and 5.0 mm in the y-direction at $t = 400$ s. The location of the interface is more precise in the x-direction because the heat is mainly transferred in the x-direction when λ is smaller than unity.
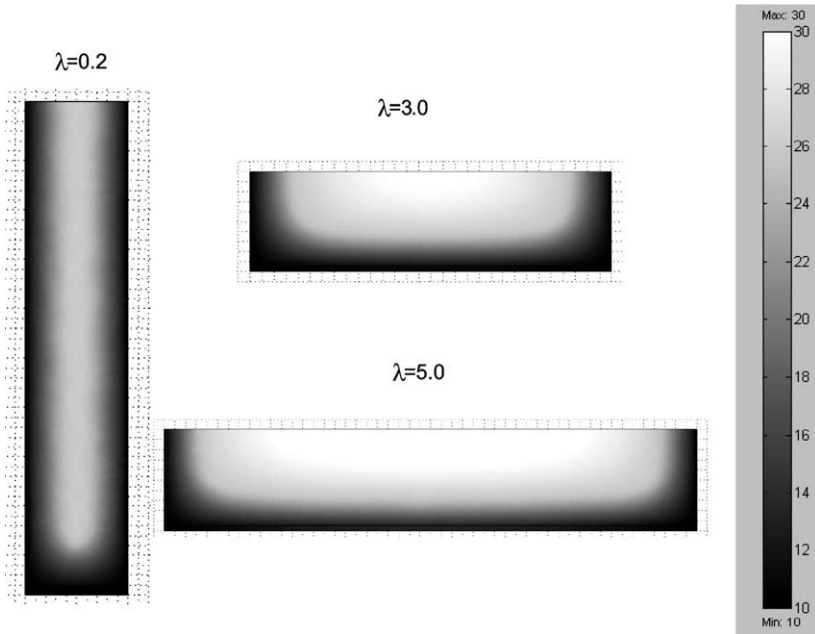
Fig. 7. The temperature distribution in the PCM store at $t = 300$ s in cases 1–3 calculated with FEMLAB by using the effective heat-capacity method.
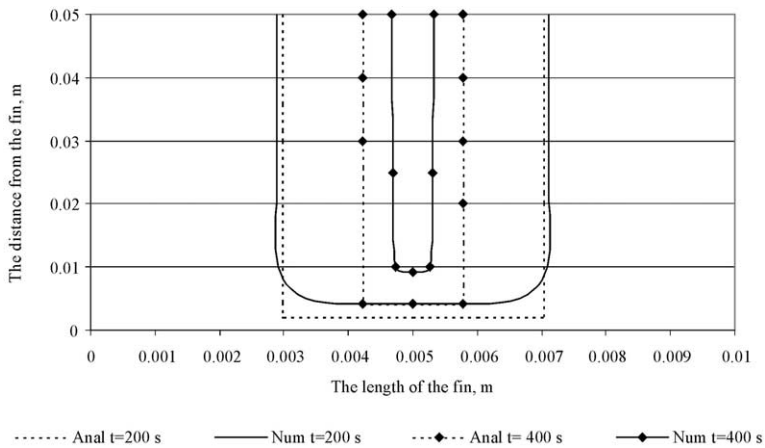
Fig. 8. The location of the solid–liquid interface computed using the analytical and the numerical solutions in case 1 ($\lambda = 0.2$, $l_f = 0.01$ m, $l_c = 0.05$ m).

The solid–liquid interface locations calculated using the derived analytical and numerical solutions at $t = 200$ s and $t = 400$ s in case 2 are presented in Fig. 9.

At $t = 200$ s the difference in the solid–liquid interface location in the x-direction is 0.1 mm and 1.1 mm in the y-direction. The numerical solution gives a rounder shape to the interface than the analytical solution because of the two-dimensional heat transfer effect in the numerical model. At $t = 400$s, the interface moves more slowly in the x-direction in the derived analytical solution than in the numerical solution. The x-directional difference between the interface location in the derived analytical and numerical solution is 1.2 mm. When the fin length increases, the assumption that the fin is initially at a lower temperature than the PCM starts to affect to the results. The difference between the interfaces is 0.6 mm where the fin length is 0.015 mm and 0.3 mm where the fin length is 0.006 mm at $t = 900$ s.

However, the analytical solution still gives a satisfactory estimation of the solid–liquid interface location.

The locations of the solid–liquid interfaces at $t = 300$ s and $t = 900$ s in case 3 are shown in Fig. 10.

The location of the solid–liquid interface in the analytical solution moves more slowly in the x-direction and more quickly in the y-direction than in the numerical solution. At $t = 300$s, the interface location difference between the analytical and numerical solution in the x-direction is 0.75 mm and 0.86 mm in the y-direction. At $t = 900$s, the interface location difference is 3.4 mm in the x-direction and 0.6 mm in the y-direction. Overall, the derived analytical solution still gives a good approximation for the solid–liquid interface location.
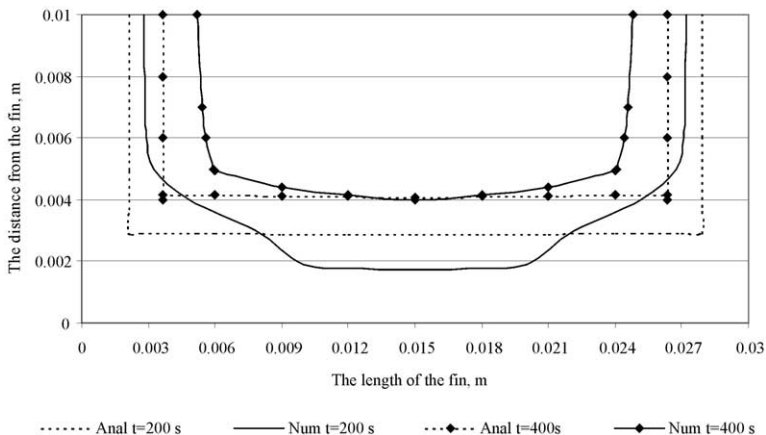
Fig. 9. The location of the solid–liquid interface in analytical and numerical solutions in case 2 ($\lambda = 3.0$, $l_f = 0.03$ m, $l_c = 0.01$ m).
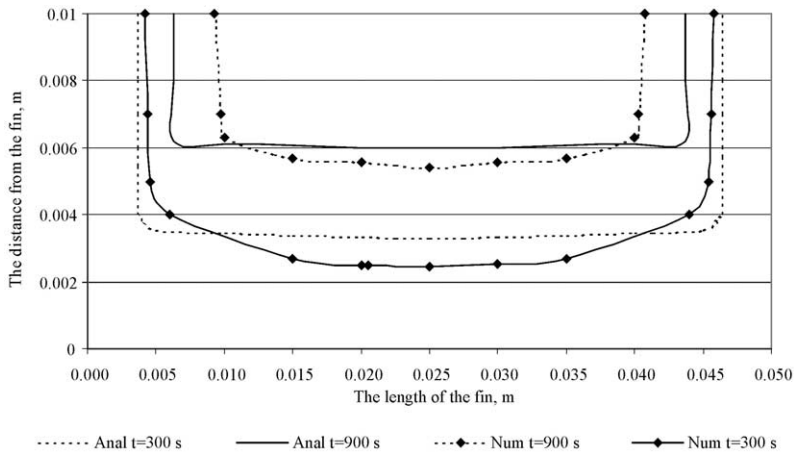
Fig. 10. The location of the solid–liquid interface in analytical and numerical solutions in case 3 ($\lambda = 5.0$, $l_f = 0.05$ m, $l_c = 0.01$ m).

5.4. Fraction of solidified PCM

Lamberg et al. [7] presented a factor called the fraction of solidified PCM, which describes how much of the storage is solidified after a certain time. The factor is given values of between zero (the store is totally liquid) and unity (the store is totally solid). The factor is defined as the volume of the solidified PCM related to the total volume of PCM in the store:

$$\varepsilon = \frac{2S_x(L_c - D - S_y) + \bar{S}_y L_f}{(L_c - D)L_f} \tag{34}$$

where $\bar{S}_y$ is the average value of the solid–liquid interface location in the y-direction along the fin length. The S_x and $\bar{S}_y$ can be calculated from Eqs. (25)–(28). The fractions of solidified PCM calculated from the derived analytical and numerical results in different test cases are shown in Table 2.

The error made in the fraction of solidified PCM, when using a derived one-dimensional analytical solution instead of two-dimensional numerical solution, is approximately ±10%. In the analytical model, it has been assumed that the solidification begins directly when $t > 0$ s. The sensible heat was taken into account in the enhanced latent-heat term. Thus, it is obvious that the analytical model over-estimated the solidification speed at the beginning of the solidification process. Later, when the time increases, the assumption that the analytical model is one-dimensional starts to affect the solidification speed and lowers it while the two-dimensional heat-transfer accelerates the speed of the solidification in the store. Nevertheless, the derived analytical model gives a good estimation for the solidification of the PCM store and the model can be used when the geometry of the store

Table 2
The fraction of solidified PCM in different test cases

	Time (s)	Rate analytical, ε_{anal} (–)	Rate numerical, ε_{num} (–)	Error $\varepsilon_{anal}/\varepsilon_{num*100\%}$
Case 1: $\lambda = l_f/l_c = 0.2$	200	0.61	0.55	5.8
	400	0.86	0.95	−9.1
Case 2. $\lambda = l_f/l_c = 3$	200	0.44	0.39	5.1
	400	0.74	0.64	−5.1
Case 3. $\lambda = l_f/l_c = 5$	300	0.45	0.38	7.3
	900	0.73	0.76	−3.3

is studied in order to find the most effective geometry for the PCM store with internal fins.

6. Discussion

The assumption that the fin is initially at the solidification temperature and the assumption that Eqs. (12)–(20) are valid when the solid–liquid interface location S_y is larger than zero, means that the model is limited to being used with pre-defined maximum fin-lengths. To find out the effect of the assumption, a numerical calculation using the effective heat-capacity method is carried out where λ is given values from 0.2 to 8.0. Fig. 11 presents the time in which the fin cools down from the initial temperature to the solidification temperature. The cooling time is presented as a function of the storage geometry.
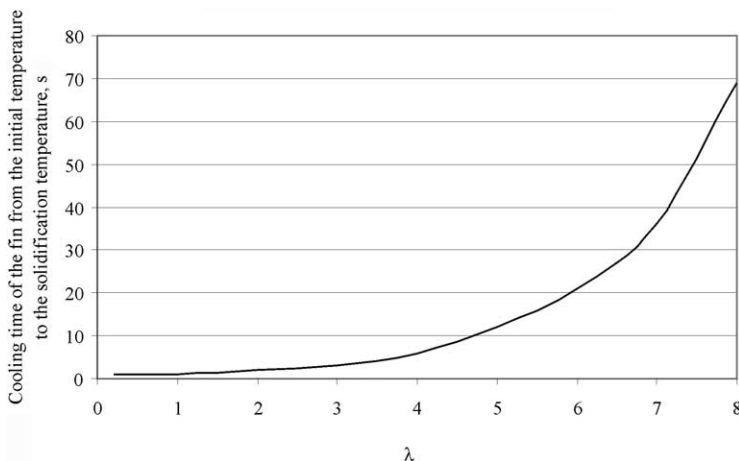
Fig. 11. Time in which the temperature of the fin achieves the solidification temperature of the fin for different geometries.

With small λ values ($\lambda = 0.3$–3.0), the cooling of the fin from the initial tempera-ture to the solidification temperature happens quickly. The cooling time is less than 3 s. When λ increases, the cooling time increases exponentially. When $\lambda = 6.0$ and the length of the fin is 0.06 m, the cooling time from the initial temperature to the solidification temperature of the PCM is 21 s.

In region 2, Eqs. (12)–(20) are valid when the $S_y > 0$. In Table 3, the solid–liquid interface locations calculated using the analytical solution at time step $t = 1$ s are presented.

It can be seen from Table 3 that when $\lambda = 6.0$ and the length of the fin is 0.06 m, the solid–liquid interface approaches the value zero. The conclusion is that the ana-lytical model is valid when $\lambda < 6.0$ and the length of the fin is $l_f < 0.06$ m.

7. Conclusions

This paper presents a simplified analytical model based on a quasi-linear, tran-sient, thin-fin equation which predicts the solid–liquid interface location and tem-perature distribution of the fin in a solidification process with a constant end-wall temperature in a finite PCM store.

The initial temperature of the fin and the PCM is assumed to be T_m instead of T_i because in this simplified model the solidification process is assumed to start imme-diately and sensible heat is taken into account in the enhanced latent-heat term—$[L + c_l(T_i - T_m)]$—which slows down the solidification front.

The following conclusions are made in relation to the accuracy of the one-dimen-sional analytical model:

- The study showed that when the width to height ratio $\lambda < 6.0$ and the length l_f of the fin was < 0.06 m, the derived analytical model is valid. The effect of the assumption that the fin is initially at the solidification temperature of the PCM on the results is small.
- At the beginning of the solidification process, the temperature of the fin is smaller for the analytical than the numerical results. The temperature dif-ference between the analytical and numerical results is greatest in the case

Table 3
The solid–liquid interface with different λ values in analytical approach at $t = 1$ s

$\lambda = l_f/l_c$	Interface location, S_y (m)
0.2	0.00021
1.0	0.00020
2.0	0.00020
3.0	0.00010
4.0	0.00002
5.0	0.00001
6.0	$\rightarrow$ 0.00000

where $\lambda = 5.0$. The assumption that the fin is initially at the PCM's solidification temperature is the reason for this phenomenon. When the time increases, the fin temperature difference between the analytical and numerical results diminishes. Overall, the analytical model gives a satisfactory result for the temperature of the fin.

- The geometry of the store has a big influence on the accuracy of the analytical model. The analytical model gives more precise results for the solid–liquid interface location in cases when λ is much smaller than unity or much bigger than unity. In these cases the heat transfer is mainly one-directional, as is the case in the derived analytical model.
- The error made in the fraction of solidified PCM when using a derived one-dimensional analytical solution instead of a two-dimensional numerical solution is approximately $\pm 10\%$. The derived analytical model gives a good estimation for the solid–liquid location in the finned PCM store and it is suitable for use in the pre-design of the PCM store.

Acknowledgements

References

[1] Peippo K. Basic thermodynamics mechanism of the phase-change material storage and energy solutions. Report TKK-F-B125. Department of Physics, 1989. [in Finnish].

[2] Velraj R, Seeniraj R, Hafner B, Faber C, Schwarzer K. Heat-transfer enhancement in a latent-heat storage system. Solar Energy 1999;65(3):171–80.

[3] Satzger P, Eska P, Ziegler F. Matrix-heat-exchanger for latent-heat-cold-storage. In: Proceedings 7th International conference on thermal-energy storage 1997. p. 307–11.

[4] Stritih U, Novak P. Heat transfer enhancement in phase-change processes. In: Proceedings Terrastock 8th International Conference on Thermal-Energy Storage, vol. 1, August 28–September 1, 2000. p. 333–8.

[5] Humphries W, Griggs E. A design handbook for phase-change thermal control and energy storage devices. NASA TP-1074, 1977.

[6] Henze R, Humphrey J. Enhanced heat-conduction in phase-change thermal-energy storage devices. International Journal of Heat and Mass Transfer 1981;24:450–74.

[7] Lamberg P, Siren K. Analytical model for melting in a semi-finite PCM storage with an internal fin. Heat and Mass Transfer 2003;39:167–76.

[8] Lamberg P, Siren K. Analytical model for solidification in a finite PCM storage with internal fins. Applied Numerical Modelling 2003;27(7):491–513.

[9] Comsol AB, FEMLAB version 2.3, reference manual, 2002.

[10] Kroeger PG, Ostrach S. The solution of a two-dimensional freezing problem including convection effects in the liquid region. International Journal of Heat and Mass Transfer 1973;17:1191–207.

[11] Rathjen KA, Latif MJ. Heat conduction with melting or freezing in a corner. Journal of Heat Transfer 1971;February:101–9.

[12] Alexiades V, Solomon AD. Mathematical modelling of melting and freezing processes. USA: Hemisphere; 1993.

[13] Carslaw H, Jaeger J. Conduction of heat in solids. 2nd ed. New York: Oxford University Press; 1959.

[14] Lamberg P, Lehtiniemi R, Henell A-M. Numerical and experimental investigation of melting and freezing processes in phase-change material storage. International Journal of the Thermal Sciences [submitted for publication].

[15] Peippo K, Kauranen P, Lund P. A multicomponent PCM wall optimized for passive solar-heating. Energy and Buildings 1991: 17(265).

[16] FEMLAB version 2.3. Comsol Oy. Lauttasaarentie 52, 00200 Helsinki, Finland. Available from: http://www.comsol.com.

[17] Incropera FP, De Witt D. Fundamentals of heat and mass transfer. Canada: John Wiley and Sons; 1990.